LETTER

doi:10.1038/nature10276

Fossil jawless fish from China foreshadows early jawed vertebrate anatomy

Zhikun Gai[1,2], Philip C. J. Donoghue[1], Min Zhu[2], Philippe Janvier[3] & Marco Stampanoni[4,5]

Most living vertebrates are jawed vertebrates (gnathostomes), and the living jawless vertebrates (cyclostomes), hagfishes and lampreys, provide scarce information about the profound reorganization of the vertebrate skull during the evolutionary origin of jaws[1–9]. The extinct bony jawless vertebrates, or 'ostracoderms', are regarded as precursors of jawed vertebrates and provide insight into this formative episode in vertebrate evolution[8–14]. Here, using synchrotron radiation X-ray tomography[15,16], we describe the cranial anatomy of galeaspids, a 435–370-million-year-old 'ostracoderm' group from China and Vietnam[17]. The paired nasal sacs of galeaspids are located anterolaterally in the braincase, and the hypophyseal duct opens anteriorly towards the oral cavity. These three structures (the paired nasal sacs and the hypophyseal duct) were thus already independent of each other, like in gnathostomes and unlike in cyclostomes and osteostracans (another 'ostracoderm' group), and therefore have the condition that current developmental models regard as prerequisites for the development of jaws[1–3]. This indicates that the reorganization of vertebrate cranial anatomy was not driven deterministically by the evolutionary origin of jaws but occurred stepwise, ultimately allowing the rostral growth of ectomesenchyme that now characterizes gnathostome head development[1–3].

A key distinction in the structure of the head of cyclostomes, in comparison with gnathostomes, is the presence of a single median duct, or 'nostril', leading to the nasohypophyseal organ, which develops from a single median nasohypophyseal placode[2,3]. The separation of the nasal and hypophyseal placodes and the development of paired, laterally located nasal sacs have been considered fundamental prerequisites for the origin of jaws, because the median position of the nasohypophyseal placode in cyclostome head development precludes the anterolateral growth of the mandibular neural crest from which a major portion of the gnathostome jaw develops[1–3].

The 420–370-million-year-old osteostracans have been regarded as the closest jawless relatives of the gnathostomes[10–13] because they share with the latter a number of uniquely derived characters, such as girdle-supported paired fins, cellular perichondral bone, a sclerotic ring and an epicercal tail[8,9]. However, their massive, mineralized braincase has a median nasohypophyseal organ resembling the condition in lampreys[8,9,18]. Consequently, osteostracans provide little insight into the evolutionary origin of jaws and speculative hypotheses of saltational evolution have therefore been proposed[19]. By contrast, the cranial anatomy of the approximately coeval galeaspids, another 'ostracoderm' group and sister relatives of osteostracans plus gnathostomes[10–13], is poorly known, despite a comparable quality of skeletal preservation[20–22].

Class Galeaspida Tarlo, 1967
Order Eugaleaspiformes Liu, 1980
Shuyu gen. nov.

Etymology. *Shu* (Chinese Pinyin): dawn; *yu* (Chinese Pinyin): fish. But essentially 'jawed fish'; thus, *Shuyu* here means 'dawn of gnathostomes'. The new genus is erected for *'Sinogaleaspis' zhejiangensis*[23,24] Pan, 1986, from the Maoshan Formation (late Llandovery epoch to early Wenlock epoch, Silurian period, ~430 million years ago) of Zhejiang, China.

Diagnosis. Small galeaspid (Supplementary Figs 6 and 7) distinct from *Sinogaleaspis* in its terminally positioned nostril, posterior supraorbital sensory canals not converging posteriorly, median dorsal sensory canals absent, only one median transverse sensory canal and six pairs of lateral transverse sensory canals[17,23].

Description of cranial anatomy. To elucidate the gross cranial anatomy of galeaspids, we used synchrotron radiation X-ray tomographic microscopy[15,16] to reconstruct seven skulls of *Shuyu*, one of the earliest and most primitive galeaspid genera. Our interpretation of the endocast is constrained by the comparative anatomy of extant vertebrates that provide a phylogenetic bracket, with hagfishes and lampreys representing a sister clade to 'ostracoderms' plus living jawed vertebrates, and with galeaspids resolved as the sister group of osteostracans plus gnathostomes[10–13,25]. The braincase of *Shuyu* is a massive endoskeletal structure that encloses the brain and sensory organs and wraps a large oralobranchial chamber ventrally (Fig. 1a, b, e, g). The cranial anatomy is inferred from the natural endocast (Fig. 1a, b) or the spaces in the endoskeleton lined post mortem with diagenetic minerals (Fig. 2a). The endocasts preserve the morphology of the brain, nerves, sensory capsules and blood vessels, which we reveal here in three dimensions. Our results confirm features of the galeaspid braincase previously reconstructed on the basis of tenuous evidence[20–22]. They also confirm the remarkable resemblance between galeaspid and osteostracan braincases, except for the arrangement of the forebrain and nasohypophyseal complex.

The galeaspids are characterized by a large median dorsal opening ('no'; Figs 1c–g and 2c–f) in the anterior part of the headshield that serves as both a common nostril and the main water intake device. Beneath the median dorsal opening is a large median oronasal cavity ('on.c'; Supplementary Figs 5 and 7) that also opens ventrally to the mouth ('m'; Fig. 3) and caudally towards the pharynx ('pha'; Fig. 3). The olfactory bulbs are housed in a pair of small fossae ('olf.b'; Figs 1c, d, g and 2a, c–f, h) that are located high in the posterior wall of the oronasal cavity and remain open anteriorly ('pr.f'; Fig. 2a–f, h). Posteriorly, the olfactory bulbs are connected to the cerebral hemispheres ('cer.h'; Fig. 2c) by paired canals for the olfactory tracts ('olf.t'; Figs 1c–e and 2c–e, h), accompanied dorsally by canals for a possible terminal nerve ('ter'; Figs 1e and 2b, h). Laterally, each olfactory bulb receives two canals from the ophthalmic artery, the anterior and posterior ethmoidal arteries ('ae.a' and 'pe.a'; Figs 1d and 2h), which are coupled with two branches of the profundus nerve ('V_1'; Figs 1c–e and 2c–e, h). Medially, the paired olfactory bulbs are separated and floored partly by an ethmoid rod ('et.r'; Figs 1d, e, g and 2a, b, h) protruding from what may correspond to the orbitonasal lamina in jawed vertebrates ('on.l'; Supplementary Fig. 5).

The nasal sacs ('na'; Figs 1c–e, g and 2b, g, h) are housed in large, paired, cone-shaped recesses located laterally in the oronasal cavity.

[1]School of Earth Sciences, University of Bristol, Bristol BS8 1RJ, UK. [2]Laboratory of Evolutionary Systematics of Vertebrates, Institute of Vertebrate Paleontology and Paleoanthropology, Chinese Academy of Sciences, Beijing 100044, China. [3]Muséum National d'Histoire Naturelle, UMR 7207 du CNRS, 47 rue Cuvier, 75231 Paris cedex 05, France. [4]Swiss Light Source, Paul Scherrer Institut, CH-5232 Villigen, Switzerland. [5]Institute for Biomedical Engineering, University and ETH Zurich, 8092 Zurich, Switzerland.

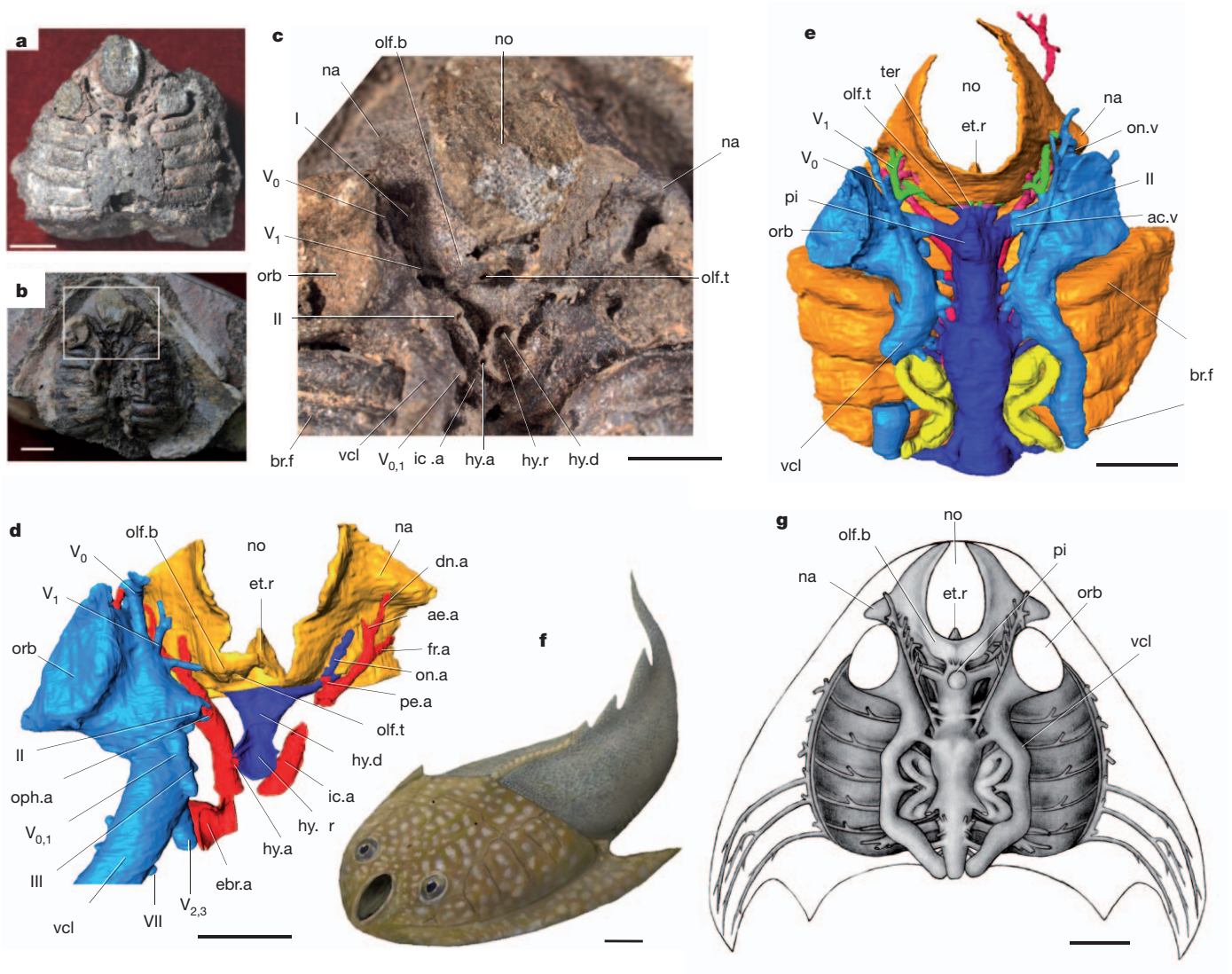

Figure 1 | *Shuyu zhejiangensis*, Silurian of Zhejiang, China. **a**, **b**, Two natural endocast specimens: V14334.1 (**a**); V14334.5 (**b**). **c**, **d**, Structure of nasal and hypophyseal region magnified from the boxed region of V14334.5: digital picture (**c**); three-dimensional (3D) reconstruction (**d**). **e**, Virtual endocast (V14334.3). **f**, Restoration of external morphology. **g**, Synthetic restoration. ac.v, anterior cerebral vein; ae.a, anterior ethmoidal artery; br.f, branchial fossa; dn.a, dorsal nasal artery; ebr.a, efferent branchial artery; et.r, ethmoid rod; fr.a, frontal artery; hy.a, hypophyseal artery; hy.d, hypophyseal or buccohypophyseal duct; hy.r, hypophyseal recess; ic.a, internal carotid artery; na, nasal sacs; no, nostril; olf.b, olfactory bulb; olf.t, olfactory tract; on.a, orbitonasal artery; on.v, orbitonasal vein; oph.a, ophthalmic artery; orb, orbital opening; pe.a, posterior ethmoidal artery; pi, pineal organ; ter, terminal nerve; vcl, lateral head vein or dorsal jugular vein; I, II, III, V_0, V_1, $V_{0,1}$, $V_{2,3}$, VII, olfactory (I), optic (II), oculomotor (III), superficial ophthalmic (V_0), profundus (V_1), superficial ophthalmic plus profundus ($V_{0,1}$), maxillomandibular ($V_{2,3}$) of trigeminal (V), and facial (VII) nerves. Scale bars, 2 mm.

Posteriorly, each nasal sac is connected to the olfactory bulb by an elongate space for the olfactory nerve ('I'; Fig. 1c) and receives two arterial canals: a dorsal nasal artery ('dn.a'; Figs 1d and 2h) branching off from the ophthalmic artery, and a ventral orbitonasal artery ('on.a'; Fig. 1d), a collateral of the internal carotid artery. Dorsally, the nasal sac is pierced by another canal for the orbitonasal vein ('on.v'; Figs 1e and 2g) that connects posteriorly to the large dorsal jugular vein ('vcl'; Fig. 1c–e, g).

The floor of the diencephalic cavity extends ventrally to form a large funnel-shaped recess for the hypophysis ('hy.r'; Figs 1c, d and 2a, b, d). The hypophyseal recess extends rostrally as a single median horizontal duct for the hypophyseal duct ('hy.d'; Figs 1c, d and 2a, b, d), which opens anteriorly to the oral cavity ('or.c'; Fig. 2a) via the hypophyseal opening ('hy.o'; Fig. 2a, b, d, f, h). The hypophyseal recess is blind caudally (Fig. 2a, b) and shows no posterior communication with the pharynx. It is flanked by a pair of large canals for the internal carotid artery ('ic.a'; Figs 1c, d and 2a, b, d, e). Laterally, it receives a minute canal for the hypophyseal artery ('hy.a'; Figs 1c, d and 2d).

Most strikingly, the paired nasal sacs of galeaspids are located laterally in the anterior part of the braincase, and the hypophyseal duct opens anteriorly and separately towards the oronasal cavity. Thus, in galeaspids these three structures are independent of each other, as in jawed vertebrates, rather than collocated, like the median nasohypophyseal complex of cyclostomes (hagfishes and lampreys) and osteostracans. Distinct, paired nasal sacs are also apparent in the extinct heterostracans[26], but the position of their hypophyseal duct is unknown. The nasohypophyseal complexes of galeaspids and hagfishes have been compared[7,8] but the arrangement of the hagfish hypophyseal duct is quite distinct, opening to the exterior via a prenasal sinus and to the pharynx caudally[27] (Fig. 3). Although the endoskeletal hypophyseal duct of galeaspids communicates with the diencephalic division of the brain cavity, the membranous duct it housed was closed

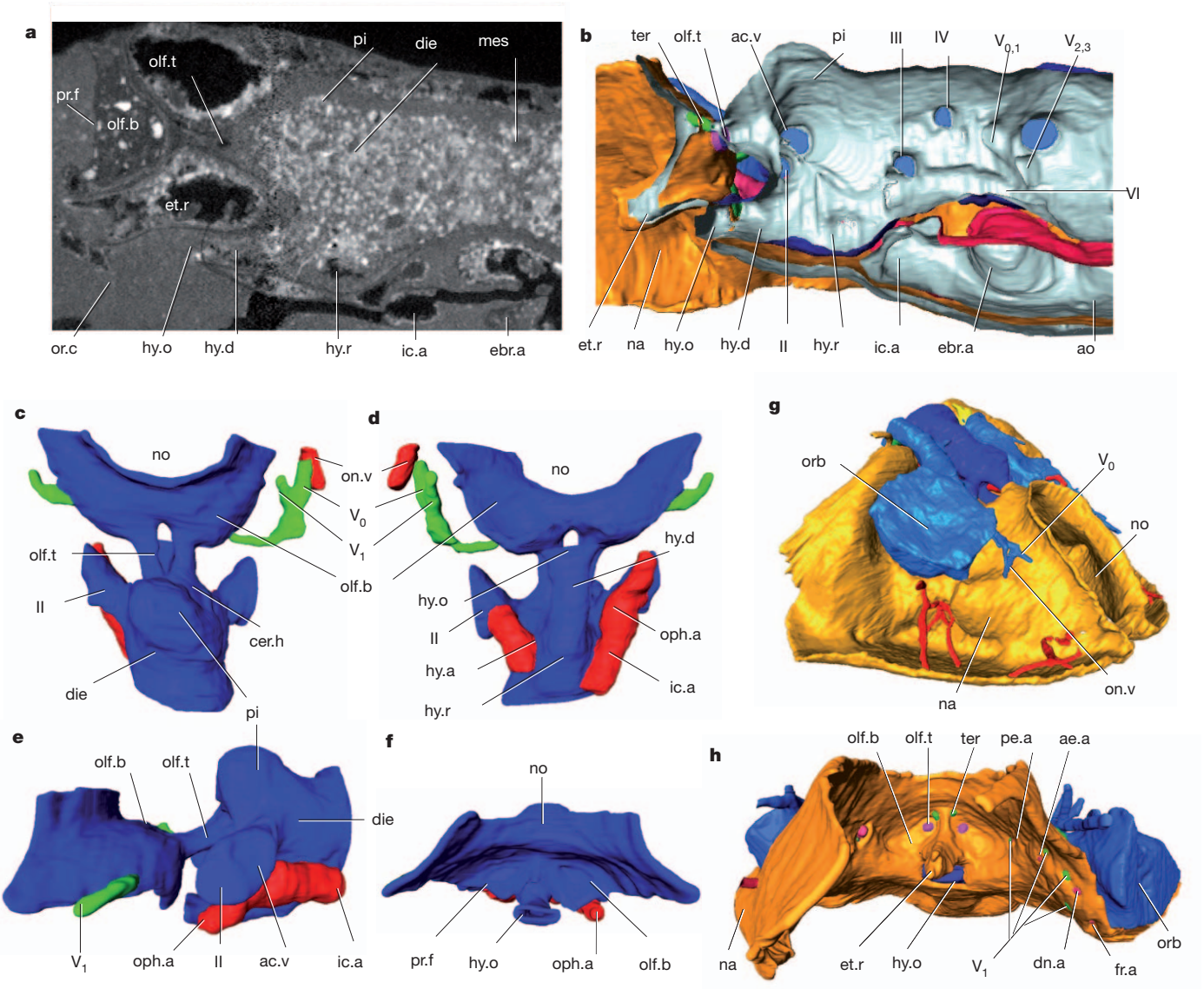

Figure 2 | The nasohypophyseal complex of *Shuyu zhejiangensis*. **a**, 512th of 1,024 sagittal slices of V14334.3, from a computerized tomography scan. **b**, Sagittal section through the braincase (V14334.3), showing the relationship between the hypophyseal duct and the nasal sacs. **c**–**f**, 3D reconstruction of the forebrain, hypophysis and related nerves and blood vessels (V14334.7): dorsal view (**c**); ventral view (**d**); lateral view (**e**); frontal view (**f**). **g**, **h**, 3D reconstruction of the nasal region: right oblique lateral view (V14334.2) (**g**); frontal view (V14334.3), showing the clear separation of the nasal sacs and the hypophyseal duct (**h**). ao, dorsal aorta; cer.h, cerebral hemisphere; die, diencephalon; hy.o, hypophyseal or buccohypophyseal opening; mes, mesencephalon; or.c, oral cavity; pr.f, precerebral fenestra; IV, VI, trochlear (IV) and abducens (VI) nerves. See Fig. 1 for other notation.

caudally, as in lampreys, osteostracans and jawed vertebrates (Fig. 3), and could not have conveyed water towards the pharynx. The hypophyseal duct of galeaspids does not show the dorsal bend seen in lampreys and osteostracans, nor the ventral orientation of the buccohypophyseal duct as in jawed vertebrates, perhaps illustrating the intermediate state from which both conditions arose.

The evolution of the nasohypophyseal complex has proven controversial because of the difficulty of distinguishing homologies from parallelisms[7,8]. However, we can now conclude that the arrangement seen in galeaspids, that is, paired nasal sacs flanking an oral cavity into which the hypophyseal duct also opens, is the shared primitive condition inherited by jawed vertebrates. This is because, at the least, separation of paired nasal sacs that seem to open towards the buccal cavity can be seen in heterostracans, the sister lineage to the clade including galeaspids, osteostracans and jawed vertebrates[10–13]. Given this framework of phylogenetic relations, the resemblance between the organization of the nasohypophyseal complex in osteostracans and that in lampreys must be a consequence of convergent evolution (Fig. 3). Osteostracans are derived, like galeaspids, from a generalized stem-gnathostome condition.

Galeaspids provide the earliest evidence for the clear separation of the olfactory organs from the hypophyseal duct in vertebrate phylogeny, a prerequisite condition in evolutionary developmental biology models for the origin of complete diplorhiny[7,8] and jaws[1–3]. Galeaspids reflect an intermediate condition in the establishment of diplorhiny and jaws in which this barrier to the forward growth of neural-crest-derived craniofacial ectomesenchyme was removed. Complete diplorhiny (nasal sacs with individual externalized nostrils) and jaws arose later in the lineage leading to the extinct placoderms and crown-group gnathostomes, but galeaspids foreshadow the stepwise assembly of these characters[8,14], in the absence of any evidence for increasingly active feeding strategies that are commonly invoked to explain the origin of the jawed vertebrates[28,29].

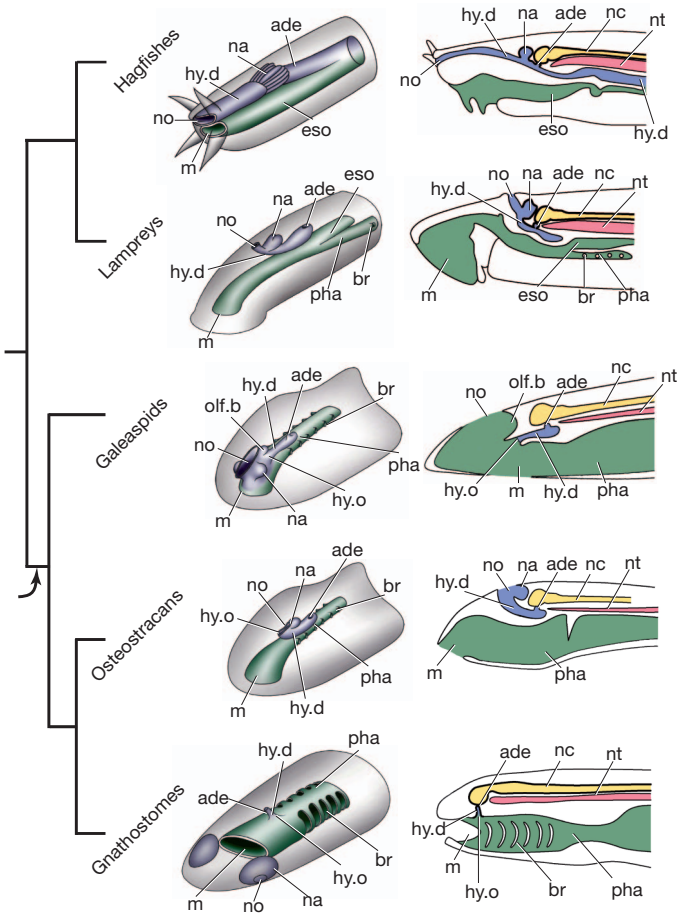

Figure 3 | The nasohypophyseal complex in craniates. Left, oblique view; right, sagittal section. The disassociation of the nasohypophyseal complex, an evolutionary prerequisite for the origin of jaws, happened at least in the common ancestor of galeaspids, osteostracans and gnathostomes (arrow). The condition of osteostracans probably converged with that of lampreys. ade, adenohypophysis; br, branchial duct or slit; eso, oesophagus; m, mouth; nc, neural cord; nt, notochord; pha, pharynx. See Figs 1 and 2 for other notation.

METHODS SUMMARY

Our investigations were performed at the TOMCAT beamline[30] of the Swiss Light Source at the Paul Scherrer Institute. The X-ray energy was optimized for maximum absorption contrast and the magnification of the X-ray microscope was ×4. Isotropic voxels of 1.85 microns were used. Projections (1,501) were acquired equiangularly over 180°, post-processed online and rearranged into flat-field- and dark-field-corrected sinograms. Reconstruction was performed on a 20-node Linux computer cluster using highly optimized filtered back-projection routines. The full volumetric information was available within a few minutes of the end of the scan. Slice data derived from the scans were then analysed and manipulated using AVIZO software (http://www.tgs.com) for computed tomography on a Hewlett Packard Workstation with a 2-GHz Intel processor and 16 GB of random-access memory. Specimens are housed in the Institute of Vertebrate Paleontology and Paleoanthropology, Beijing.

Received 16 February; accepted 7 June 2011.

1. Kuratani, S. & Ota, K. G. Primitive versus derived traits in the developmental program of the vertebrate head: views from cyclostome developmental studies. *J. Exp. Zool.* **310B,** 294–314 (2008).
2. Kuratani, S., Nobusada, Y., Horigome, N. & Shigetani, Y. Embryology of the lamprey and evolution of the vertebrate jaw: insights from molecular and developmental perspectives. *Phil. Trans. R. Soc. B* **356,** 1615–1632 (2001).
3. Uchida, K., Murakami, Y., Kuraku, S., Hirano, S. & Kuratani, S. Development of the adenohypophysis in the lamprey: evolution of epigenetic patterning programs in organogenesis. *J. Exp. Zool.* **300B,** 32–47 (2003).
4. Shigetani, Y. *et al.* Heterotopic shift of epithelial-mesenchymal interactions in vertebrate jaw evolution. *Science* **296,** 1316–1319 (2002).
5. Khonsari, R. H., Li, B., Vernier, P., Northcutt, R. G. & Janvier, P. Agnathan brain anatomy and craniate phylogeny. *Acta Zool.* **90,** 52–68 (2009).
6. Smeets, W. J. A. in *The Central Nervous System of Vertebrates* (eds Nieuwenhuys, R., ten Donlelaar, H. J. & Nicholson, C.) 551–654 (Springer, 1998).
7. Janvier, P. *Early Vertebrates* (Clarendon, 1996).
8. Janvier, P. in *Major Events in Early Vertebrate Evolution* (ed. Ahlberg, P. E.) 172–186 (Taylor and Francis, 2001).
9. Janvier, P. in *Major Transitions in Vertebrate Evolution* (eds Anderson, J. S. & Sues, H.-D.) 57–121 (Indiana Univ. Press, 2007).
10. Janvier, P. The dawn of the vertebrates: characters versus common ascent in the rise of current vertebrate phylogenies. *Palaeontology* **39,** 259–287 (1996).
11. Forey, P. L. & Janvier, P. Agnathans and the origin of jawed vertebrates. *Nature* **361,** 129–134 (1993).
12. Forey, P. L. Agnathans recent and fossil, and the origin of jawed vertebrates. *Rev. Fish Biol. Fish.* **5,** 267–303 (1995).
13. Donoghue, P. C. J. & Smith, M. P. The anatomy of *Turinia pagei* (Powrie) and the phylogenetic status of the Thelodonti. *Trans. R. Soc. Edinb. Earth Sci.* **92,** 15–37 (2001).
14. Donoghue, P. C. J. & Purnell, M. A. Genome duplication, extinction and vertebrate evolution. *Trends Ecol. Evol.* **20,** 312–319 (2005).
15. Donoghue, P. C. J. *et al.* Synchrotron X-ray tomographic microscopy of fossil embryos. *Nature* **442,** 680–683 (2006).
16. Tafforeau, P. *et al.* Applications of X-ray synchrotron microtomography for non-destructive 3D studies of paleontological specimens. *Appl. Phys. A* **83,** 195–202 (2006).
17. Zhu, M. & Gai, Z.-K. Phylogenetic relationships of galeaspids (Agnatha). *Vertebr. PalAsiat.* **44,** 1–27 (2006).
18. Stensiö, E. A. *The Downtonian and Devonian Vertebrates of Spitsbergen. Part 1: Family Cephalaspidae.* (Arno, 1927).
19. Mazan, S., Jaillard, D., Baratte, B. & Janvier, P. *Otx1* gene-controlled morphogenesis of the horizontal semicircular canal and the origin of the gnathostome characteristics. *Evol. Dev.* **2,** 186–193 (2000).
20. Halstead, L. B. Internal anatomy of the polybranchiaspids (Agnatha, Galeaspida). *Nature* **282,** 833–836 (1979).
21. Halstead, L. B., Liu, Y.-H., & P'an, K. Agnathans from the Devonian of China. *Nature* **282,** 831–833 (1979).
22. Wang, N.-Z. in *Early Vertebrates and Related Problems in Evolutionary Biology* (eds Chang, M.-M., Liu, Y.-H. & Zhang, G.-R.) 41–65 (Science Press, 1991).
23. Gai, Z.-K., Zhu, M. & Zhao, W.-J. New material of eugaleaspids from the Silurian of Changxing, Zhejiang, China, with a discussion on the eugaleaspid phylogeny. *Vertebr. PalAsiat.* **43,** 61–75 (2005).
24. Pan, J. in *Professional Papers Presented to Professor Yoh Sen-shing* 67–75 (Geological Publishing House, 1986).
25. Heimberg, A. M. Cowper-Sal·lari, R. Sémon, M., Donoghue, P. C. J. & Peterson, K. J. MicroRNAs reveal the interrelationships of hagfish, lampreys, and gnathostomes and the nature of the ancestral vertebrate. *Proc. Natl Acad. Sci. USA* **107,** 19379–19383 (2010).
26. Janvier, P. & Blieck, A. New data on the internal anatomy of the Heterostraci (Agnatha), with general remarks on the phylogeny of the Craniota. *Zool. Scr.* **8,** 287–296 (1979).
27. von Kupffer, C. *Studien zur Vergleichenden Entwicklungsgeschichte des Kopfes der Kranioten. Heft 4: Zur Kopfentwicklung von Bdellostoma* (Lehmann, 1900).
28. Gans, C. & Northcutt, R. G. Neural crest and the origin of the vertebrates: a new head. *Science* **220,** 268–273 (1983).
29. Baker, C. V. H. & Schlosser, G. The evolutionary origin of neural crest and placodes. *J. Exp. Zool.* **304B,** 269–273 (2005).
30. Stampanoni, M. *et al.* TOMCAT: a beamline for tomographic microscopy and coherent radiology experiments. *Synchr. Radiat. Instrum.* **879,** 848–851 (2007).

Supplementary Information is linked to the online version of the paper at www.nature.com/nature.

Acknowledgements We thank F. Marone, S. Bengtson, E.-M. Friis, N. J. Gostling, T. Huldtgren, M. Pawlowska and C.-W. Thomas for assistance in retrieving synchrotron radiation X-ray tomographic microscopy data; Q.-S. Chen and W.-J. Zhao for field work; and S. Powell, F.-X. Wu, B. Choo and R.-D. Zhao for illustrations. This work was supported by the Chinese Academy of Sciences (KZCX2-YW-156), the Chinese Foundation of Natural Sciences (40872020, 40930208), the Major Basic Research Projects (2006CB806400) of MST of China, the Paul Scherrer Institut (P.C.J.D.), European Union FP6 (P.C.J.D.), the Leverhulme Trust (P.C.J.D.), the Natural Environmental Research Council (P.C.J.D.), the SYNTHESYS Project (Z.G.) and a Dorothy Hodgkin studentship from the Royal Society (Z.G.).

Author Contributions P.C.J.D. and M.Z. designed the project. Z.G. performed the research and led the writing of the manuscript. P.C.J.D., M.S. and Z.G. conducted the synchrotron radiation X-ray tomographic microscopy. All authors discussed the results and wrote the manuscript.

Author Information Reprints and permissions information is available at www.nature.com/reprints. The authors declare no competing financial interests. Readers are welcome to comment on the online version of this article at www.nature.com/nature. Correspondence and requests for materials should be addressed to P.C.J.D. (phil.donoghue@bristol.ac.uk) or M.Z. (zhumin@ivpp.ac.cn).